LAWRENCE
LIVERMORE
NATIONAL
LABORATORY

LLNL-JRNL-416422

What Can We Learn From The Shape Of A Correlation Peak For Position Estimation?

A. A. S. Awwal

September 1, 2009

Applied Optics

Disclaimer

What can we learn from the shape of a correlation peak for position estimation?

Abdul Ahad S. Awwal

National Ignition Facility, Lawrence Livermore National Laboratory, Livermore, CA 94551

[*]Corresponding author: awwal1@llnl.gov

Matched filtering is a robust technique to identify and locate objects in the presence of noise. Traditionally, the amplitude of the correlation peak is used for detection of a match. However, when distinguishing objects that are not significantly different or detecting objects under high noise imaging conditions, the normalized peak amplitude alone may not provide sufficient discrimination. In this paper, we demonstrate that measurements derived from the shape of the correlation peak offer not only higher levels of discrimination but also accurate position estimation. To our knowledge, this is the first time such features have been used in a real-time system, like the National Ignition Facility, where such techniques enable real-time, accurate position estimation and alignment under challenging imaging conditions. It is envisioned that systems utilizing matched filtering will greatly benefit from incorporating additional shape based information.

OCIS codes: 070.0070, 100.0100, 070.5010, 100.2000, 100.3008, 100.4999, 100.5010, 150.5758, 220.1140, 350.4600, 140.3538, 350.266, 140.0140

1. Introduction

Matched filtering or cross-correlation offers a robust approach for identification of objects in the presence of noise. Traditionally, the amplitude of the correlation peak is used for detection of a known object present in an image. However, when a different object with similar shape is correlated, the reduction in magnitude of the correlation peak may not provide an adequate indication of this difference. This fact poses a problem in the detection of objects that may be slightly different. One way to enhance the discrimination is to normalize the correlation output with respect to the total output in the correlation plane. This normalized correlation peak indicates the percentage of the total power in the correlation plane that is concentrated in the correlation peak.

The National Ignition Facility (NIF), constructed at the Lawrence Livermore National Laboratory, is a stadium-sized facility containing a 192-beam, 1.8-megajoule, 500-terawatt, ultraviolet laser system for the study of inertial confinement fusion and the physics of matter at extreme temperatures and pressures [1]. Automatic alignment (AA) based on computer analysis of fiducials in video images [2,3] enables scientists to direct all 192 high-energy laser beams with precise alignment to produce temperatures approaching 100 million K and pressures at 100 billion atmospheres, conditions which are designed to achieve ignition of a deuterium-tritium (DT) fusion target [4]. NIF also serves as a real-time large-scale repository of laser images, which are archived and available for testing and development of new detection algorithms for off-normal cases.

In NIF, matched filtering is used to determine the position of fiducials in a number of beam images for alignment purposes. Without defining high-power pulsed laser components, these images fall into several categories including various pinhole images [5-7], fiducials in the shape of squares and circles in the pre-amplifier module [8], corner-cube reflected pinhole images [9], back-reflection images from frequency-doubling crystal made of potassium di-hydrogen phosphate (KDP) [10], programmable spatial shaper images and most recently "active target images" with extremely low-contrast fiducials. Some of the templates used to detect these images are generated analytically while others are generated from real images. For example, the template for pinhole images is generated analytically [6,7,9], while those for the KDP [10] and some of the corner-cube pinhole images [5] are generated from a set of real images for each beam line. For KDP images, all 192 of the beam templates are not only different [10] but they change over time. In some instances, the beam profile changes drastically due to the application of a phase plate (required to deliver more uniform energy to the mm-sized target). In all these cases, this difference in beam shape must be detected, otherwise serious position error will result. In some other instances, various structural noise may appear in an image, where a high normalized correlation output may actually lead to a position error. Sometimes, the noise may be too strong compared to the signal strength, so that choosing the magnitude of the correlation may lead to a complete misidentification. Therefore, the need for a more reliable method for identification of a match under all such conditions is of paramount importance.

In this work, we propose to utilize shape-based correlation metrics instead of magnitude-based correlation metrics alone to enhance detection and position accuracy. We demonstrate the application of shape-based technique for (a) detecting small changes in the beam template, (2) detecting proper position estimation in very challenging imaging conditions, (3) determining

autonomous switching algorithm, and (4) detecting extremely-low-contrast objects in the presence of high contrast noise. We also show that some features of the correlation shape increases the discrimination efficiency for both classical matched filtering and the amplitude modulated phase only filter. In other cases, we show when to reject a maximum correlation peak in favor of a properly-shaped correlation peak for better position estimation. To our knowledge, this is the first time such features have been used in a real-time system like NIF for matched-filter-based position determination. After the algorithm section, we introduce some of the shape features currently in use for various position detection algorithms at NIF. Then we summarize our main results from these various image processing applications at NIF where the shape-based features play crucial roles.

2. Algorithm

The *classical matched filter* (CMF) introduced by VanderLugt [11] for optical pattern recognition, stores the complex amplitude and phase of the reference pattern as a hologram. The *phase only filter* (POF), a variation of the CMF, exploits only the phase of the reference pattern to accomplish correlation recognition [12]. The amplitude modulated phase only filter (AMPOF) [13] was designed to further enhance the performance of the POF. The mathematical formulation of the AMPOF filter can be derived in the following manner by modifying the amplitude of the CMF. Let the Fourier transform of the object function f(x,y) be denoted by:

$$F(U_x, U_y) = \left|F(U_x, U_y)\right| \exp(j\Phi(U_x, U_y)) \tag{1}$$

The CMF corresponding to this function f(x,y), according to the Fourier transform theory of correlation, is simply the complex conjugate of the Fourier spectrum as denoted by Equation 2.

$$H_{CMF}(U_x,U_y) = F^*(U_x,U_y) = \left|F(U_x,U_y)\right|\exp(-j\Phi(U_x,U_y)) \quad (2)$$

The inverse Fourier transformation of the product of $F(U_x, Uy)$ and $H_{CMF}(U_x, Uy)$ leads to the convolution of $f(x, y)$ and $f(-x, -y)$, which is the equivalent of the auto-correlation of $f(x, y)$. Moreover, when $|F(U_x, Uy)|$ is set to unity, H_{CMF} becomes a *phase only filter* (POF) as shown in Equation 3.

$$H_{POF}(U_x,U_y) = \exp(-j\Phi(U_x,U_y)) \quad (3)$$

Since the convolution operator in the spatial domain is equivalent to the product operator in the frequency domain, one can think of the POF as an edge enhancer by way of division by $| F(U_x, U_y) |$. To get a sharper peak, it is instructive to divide the H_{POF} by a magnitude function, which will lead to an impulse type of correlation. The generalized AMPOF utilizes a polynomial to perform the division is expressed as [14]:

$$H_{AMPOF}(U_x,U_y) = \frac{aF^*(U_x,U_y)}{\left[\ b + c\left|F(U_x,U_y)\right| + d\left|F(U_x,U_y)\right|^2\ \right]^m} \quad (4)$$

Constants a,b,c, and d can be chosen to achieve various forms of AMPOF, CMF or POF. Thus when, a = b = m = 1, c = d = 0, it results in the classical matched filter; when b = d = 0, a = c, m = 1 it results in a phase only filter. When b is a small constant for nonzero values of a, c, and d it is an AMPOF. The AMPOF described in [13] has a = constant, d = constant, c = 0, m = 1 and b = ε (a small constant number). It was found, after some experimentation, that when b = ε, d = 0 and c = a = 1, better stability of position detection results in the KDP beam image. More detailed optimization of these parameters is possible [15,16]. The AMPOF correlation of the input image and the target is simply:

$$C_{AMPOF}(\Delta_x,\Delta_y) = F^{-1}\{F(U_x,U_y)H_{AMPOF}(U_x,U_y)\} \quad (5)$$

3. Correlation-shape-based metrics

When performing position estimation using a matched filter, various aspects of correlation shape can be indicators of a desirable best match and hence the best estimated position. In this section, we introduce various parameters related to correlation shape. These parameters range from an aspect of the correlation peak such as its sharpness or lack of it, to the shape of the whole correlation plane. In addition, we include some commonly used performance criteria.

A. Pedestal

The sharpness (or broadness) of the correlation peak is an indicator of good match. We define the sharpness (or lack of it) by the broadness of the correlation peak using a measurement we call pedestal

$$\text{Pedestal} = \sum C(x,y) \ > T \quad (6)$$

where T = fraction * max(C(x,y)). Typical values of fraction considered are 0.5 or 0.9 in this paper. Also note that since the "greater than" operation produces a True or False answer, the pedestal is the sum of the number of pixels that exceeds 50% or 90% of the peak value.

B. Discrimination ratio

The discrimination ratio is used as a measure of performance to compare different metrics. It is defined as the difference between auto- and cross-correlation parameters expressed as a percentage of the auto-correlation parameter. Practically, a higher discrimination ratio provides a threshold that is easy to implement. A lower discrimination means that whatever threshold is

selected needs to be carefully maintained and adjusted as necessary with changing operational conditions. Discrimination ratio (DR) is defined as

$$DR = \frac{\text{Abs(Auto correlation parameter - cross correlation parameter)}}{\text{Auto correlation parameter}} \tag{7}$$

C. Normalized peak

The normalized peak (NP) is defined as the

$$NP = \frac{\max\,(C(x, y))}{\sum C(x, y)} \tag{8}$$

In the energy domain, a similar metric is defined where a squaring operation is performed, which is known as peak-to-correlation energy (PCE) [18]. The numerator in the above metric is known as the absolute peak. In the context of the present work, normalized peak is used to identify possible candidates of match, other metrics are used to qualify (accept or reject) that particular match.

D. Mean square error (MSE) in shape

When detecting the best correlations in extremely challenging situations, such as very high background noise with negligible object contrast, the shape around the correlation peak is compared to the auto-correlation shape. The best match is said to be with the lowest MSE which is defined as error below:

$$MSE = \frac{\sum (\text{auto} - \text{cross})^2}{n \times n} \tag{9}$$

Where the auto (cross) represents the nxn pixels around the auto (cross) correlation peaks. When subimaging is used, nxn could extend to the dimension of the whole subimage.

E. Variance in inverse shape metric

Sometimes MSE alone may not provide a strong indication of match. When a dot product of the inverse of the cross-correlation with the auto-correlation is performed, the product will lead to a matrix filled with unity, in case there is a perfect match. Any deviation from the constant magnitude is an indication of mismatch. Therefore the standard deviation (stddev) of this product is used to measure the similarity. A lower value of the standard deviation indicates a higher degree of match in the shape. It is possible that the cross-correlation may have zeros. Therefore, practically, when calculating the inverse, only those elements are included that give a non-zero denominator.

$$\text{error} = \text{stddev}\frac{\text{auto}}{\text{cross}} \tag{10}$$

F. Double peak

When detecting a single object in a scene, a single peak is expected. However, due to various optical disturbances such as wavefront distortion, one may get images which contain an overlap of a slightly displaced multiple objects or artifacts which can create impression of a false object. This shows up as double peak in the correlation plane. If we choose one of the two peaks, the position estimation is biased. Therefore, when selecting the best match, a double peak is to be avoided. In the following sections, we describe how correlation-shape-based criteria are used to achieve accurate and reliable position estimation.

4. Numerical Experiment with synthetic data

In order to illustrate the effectiveness of these proposed metrics, a simple experiment utilizing two very similar-shape synthetic objects is conducted to compare one of the shape-based metrics,

namely the pedestal, to normalized correlation peak in terms of discrimination ratio. The two objects are a circle and an octagon as shown in Fig. 1; the diameter of the circle is equal to the distance between the parallel sides of the octagon. These experiments precede the applications involving real NIF images described in the following sections, and they provide an understanding of the magnitude of effectiveness of this correlation shape-based approach.

Each of the two objects is used as a template in the CMF and AMPOF formulation, thus allowing us to compute and compare both auto- and cross-correlation measurements and hence determine the discrimination efficiency. First, a CMF is formulated with the circle object and matched against both the circle and the octagon input. As the circle is smaller than the octagon, the region of maximum overlap occurs when the circle overlaps with itself or with the octagon.

The normalized auto-correlation provides us with a discrimination of 9.8% while the pedestal measurement provides discrimination of 47%-112% as shown as shown in Table I (exp. 1). Note also that as expected with a circle filter (which completely overlaps with the octagon), the absolute correlation peak is exactly the same for both auto- and cross-correlation. On the other hand, if we use the octagon object as the filter (Exp. 2, Table I), normalized auto-correlation provides a 0.31% discrimination while the pedestal approach yields 18% - 264%! The absolute peak in this case, however, provides some discrimination. Since the octagon area is larger than the circle, it provides a higher auto-correlation value, resulting in 9.3% discrimination in the absolute peak value. Fig. 2 depicts the auto- and cross-correlation outputs with the octagon as matched filter.

Next we formulate the AMPOF filters (Exp3. and Exp. 4). We see a dramatic improvement of the discrimination ratios in the pedestal measurement is observed compared to the CMF, which ranges from several hundred to several thousand! The dramatic change in the

cross-correlation width is evident from the AMPOF outputs shown in Fig. 3. Additionally, in the AMPOF, the discrimination ratio of the peak or normalized peak, is improved to over 60% compared to DR of under 10 for CMF. Note that all discrimination ratios are expressed as a percentage calculated by normalizing the difference between auto- and cross-parameters (pedestal, peak etc.) by the auto parameters. Also to be noted is that pedestal at 0.5 (or 0.9) counts all the pixels that exceed 50% (or 90%) of the peak value in the correlation plane. The normalized peaks are multiplied by 10^5 to make all normalized quantities in the same scale.

To make the simulation more realistic, noise is added to the images. Noise with standard deviation of 25 and 100 was added to the input images. From Exp 5 and 6 it is noted that while the DR of pedestal is slightly reduced from 112% to 73%, the negative discrimination is observed in the case of absolute peak values. The negative DR indicates that the cross-correlation value is greater than the auto-correlation. This will be equivalent to a false match. The normalized peaks however maintain a positive discrimination. For AMPOF, DR again reduces slightly but has more than 10 times the value of NP or AP. Very similar trends are observed when the octagon is used as the filter. Fig. 4 illustrates the relative magnitude of DR for various schemes.

5. Real-time matched filtering for NIF automatic alignment

Accurate, fast and robust beam position detection is one of the objectives of the automatic alignment (AA) image processing at NIF. The NIF laser is aligned by adjusting the laser optics at various control points along the beam path. The AA system autonomously operates 35,000 computer-controlled devices, such as motorized actuators and video cameras, to adjust mirrors and other optics. It currently performs 26 separate optical adjustments on each of the 192 NIF beams in less than 15 minutes [8]. In these control points, various fiducials are used to align the

beam. For example, in the pre-amplifier module [5] geometric patterns (e.g., small circles or squares) imprinted on optical components identify the beam and reference positions. In other cases, it is simply Gaussian beams produced by fiber light source.

5.1 KDP – Detecting correct template

In KDP alignment, the back reflection from the KDP frequency conversion crystal is used for aligning the crystal angle necessary for producing maximum gain. Template matching has been used as one of the approaches to align the KDP crystal. The templates for each beam are generated by averaging co-registered beam images acquired over several months.

Two scenarios require us to identify that a specific beam is using its correct template. The first case is when a beam is accidently using a template from another beam line. Secondly, the template belongs to the correct beam, but the beam shape has changed over time. Both of these cases can produce highly unpredictable results. In the first case, the wrong template must be detected and alignment stopped for a human operator intervention; in the second case, we need to update our template to permit matching with the current beam shape and maintain high stability of beam position. The template update requires us to detect the situation as soon as the beam shape starts changing, which may be a very small change. It was found that the normalized correlation peak is not able to detect small changes in back reflection patterns. Practically, it is hard to come up with a detection threshold that will work with various images under varying illumination conditions. Experiments with various types of matched filtering demonstrated that the AMPOF filter resulted in good detection stability [10] with an extremely narrow auto-correlation peak. The following experiment demonstrates how the pedestal can provide enough discrimination to detect small difference in beam characteristics. The template for one of the beam lines was used to correlate with three other beam lines representing out-of-class images.

Then noise of various magnitudes and types were added to the beam image corresponding to the template to create realistic scenarios for in-class image. Table I lists the pedestal for in class and out-of-class images.

For the auto-correlation case, the pedestal of the auto-correlation peak is very low, signifying a very narrow peak. However, for the images that are significantly different than the template, the pedestal is high. The noisy images exhibit wider peaks or many false peaks, which increase the pedestal. Analyzing Table II, a correlation peak with a pedestal above 160 was considered reasonable to detect all similar-class images but reject all of the out-of-class images. However, since the real images are not as noisy as those simulated ones, a smaller threshold of 100 was found very practical. This ensures that when the beam pattern starts to change, change in pedestal can be detected. When the change exceeds the threshold, a new template must be calculated.

5.2 KDP – phase plate: automatic algorithm switching

When a phase plate is introduced into a beamline to distribute the intensity more evenly, the image loses its structural pattern and appears rather like a diffused area of speckled intensity. In such cases, the pedestal increases to several hundred reaching a value of 800 or above. Thus it is simple to detect this condition and switch to a different algorithm. The matched filtering algorithm does not work since the speckled intensity cannot be correlated to any specific pattern. The alternate algorithm applies a dilation operator multiple times to grow a binary mask which fits the region of the illuminated areas. Then a weighted centroid is performed on that region. By eliminating noisy pixels from outside the region of interest using the dilated mask, a stable measurement is achieved.

5.3 Corner cube pinhole images – search for radius

The corner cube pinhole image appears in one crucial part of the NIF laser alignment. This image is created by light from two fiber sources bouncing of the corner-cube mirror and coming to a common overlap. When the wavefront correction is performed properly, the image appears to be very crisp and of high quality with clearly defined diagonal lines and circular outline. When wavefront or other distortions exist, various artifacts appear in the image to create false edges (as seen in Fig. 5) or a secondary shadow, or two almost equally bright pinholes displaced with respect to each other.

Currently, a matched filter is used to detect the center of the beam. To enhance the correlation performance, the edge of a perfect disc is used as a template and matched against the edge of the pinhole image. Since the size of the pinhole may vary due to magnification and focus, a search algorithm is executed to find the best circle to match the outer perimeter of the pinhole. For a good quality image, choosing the maximum of the normalized peak is sufficient to provide a good position estimate. However, when the quality deteriorates, the position using the normalized peak alone gives rise to a biased estimate. When the images have a shadow or edge artifact, it is possible to have the estimate biased towards one of the false edges. In the case where there are multiple pinholes, the result could bias towards the brighter pinhole. The desired position is usually the center of the biggest possible circular image, or the center of the multiple overlapped pinhole images. Note that a centroiding does not work very well in these situations. Since the images suffer from significant beam non-uniformity, any attempt to clean the image may result in significant loss of beam area.

For finding a better position estimation, multiple criteria are used to select the best match circle. We keep track of the maximum correlation peak as well as several features of the

correlation shape, such as pedestal and number of peaks. Specifically, we exclude any measurement that displays a double peak indicative of a match with two distinct circles. Whenever a maximum correlation is selected at a double peak, the corresponding position shows that it has selected one of the two circles or latched into a shadow artifact. If a maximum correlation peak is obtained with a minimum pedestal, it is an indication of a good match.

Note from Fig. 5 that the maximum of normalized peak is detected at radius 36. The corresponding position shows that the circle with this radius matched with the right edge of the image and an inner dark edge on the left, which is not a true edge. The position estimate was rejected by careful examination of the correlation shape. As shown in Fig. 6(a-b), a double peak is observed, therefore this maximum was skipped to look for a better-shaped correlation peak. Finally at radius 41 another correlation maximum was obtained with a nice single peak with a minimum of the pedestal. This example demonstrates use of multiple shape-based criteria to choose a good position estimate.

5.4 Subimaging in high background images – rejecting false matches

In infrared images with very bright backgrounds the object appears to be very dim. In ref. [8] we show that the normalized correlation peak is not able to detect a match with the very faint object for target tracking application. In fact, cross-correlation appears to be higher than the auto-correlation. The real target was detected by comparing the whole correlation plane output from the subimage to the auto-correlation function of the target image. In other words, it compares the whole shape of the sub-image correlation to the shape of the auto-correlation to determine the match. If C(x,y) is the auto-correlation and G(x,y) is any correlation output, then min(C(x,y)-G(x,y)) is used to detect the match. For practical purposes, a threshold may be used to detect that the difference is below some real number.

5.5 Detecting extremely low-contrast objects with high background noise

When an object of interest has a low signal-to-noise ratio, selecting the highest correlation is not effective. Rather, the highest peaks act as traps for false detection. Examples of such images, shown in Fig. 7 and 9, are the active target images used for automatic alignment of the target camera in the NIF target chamber. The image is of the CCD array itself, with fiducials etched into the CCD. Two different views of this CCD array are taken by two different cameras. In a top view, the faint fiducials are shown as flat elliptical objects as shown in Fig. 7(a). In the second type of view as shown in Fig. 9(a), the observing camera is at an oblique angle of nearly 15 degrees. Thus the same fiducials now appear to be much smaller. The noise is amplified, while the fiducial loses its contrast due to the small angle of observance. In both cases, the fiducials of interest are of extremely low intensity and contrast with very bright noise in the background. The second image shows that many parts of the image have very similar features as the faint fiducials. The highest correlation peaks are generated by the bright noise sources.

A template is formed by selecting a fiducial from one of the real images as shown in Fig. 7(b). When correlated with image in Fig. 7(a), the resulting correlation plane output shown in Fig. 7(c) shows a large number of peaks corresponding to many false matches. Note that we removed the bright lines in the preprocessing stage. To separate the false peaks from the real peaks, first the auto-correlation peak is generated from the template as shown in Fig. 8(a). Then a segment is cut around the auto-correlation peak and used as a template for difference comparison as shown in Fig. 8(b). It is compared to the first peak in Fig. 8(c). Since the difference is smaller than a specified threshold, it is accepted. The next two peaks as shown in Fig. 8(d-e) turn out to be false peaks. Finally the second peak is detected as shown in Fig. 8(f). If the processing steps

do not remove all the brighter noise, as high as 30 false peaks may have to be discarded before finding all the real peaks.

The active target side images as shown in Fig. 9(a) offer the most difficult challenge. Note that when a template generated from a real image is used as a matched filter, a huge number of false peaks appear in the correlation plane. Also the challenge is exacerbated by the fact that the contrast of the target is absolutely low in the presence of many high contrast features of various sizes in the image. To enhance the correlation performance in both of these active target images, filtered edge images generated from the real images are used as a template.

The segmented auto-correlation is shown in Fig. 10(a). In the case of a side image in Fig. 9(a) however, the MSE criteria did not work to provide sufficient discrimination. The true match was identified using the standard deviation of the product of inverse. In some images, the true peaks may be identified after 90 or more correlation comparisons. The shape of the correlation is exploited to filter out a valid match from hundreds of invalid matches. Using the information from self-correlation, we are able to avoid false matches and find the best match under very challenging lighting conditions.

6. Conclusion

Matched filtering is a powerful position estimator for of discrete objects in an image with noise. While the normalized correlation peak and other metrics have been proposed in the literature, the focus of this work has been more on the shape aspect. The specific method of combining these two aspects of the correlation plane output, magnitude and shape [19-21], may ultimately determine the success of the matched filtering in a particular situation. We demonstrated the role of the pedestal in detection of small or large deviation in shape, double peaks in avoiding biased estimates, and deviation from auto-correlation shapes to detect extremely low contrast objects.

Some of the challenges we face at NIF in terms of real-time signal processing allow us to discover more interesting aspects of this problem of position detection.

Acknowledgement

This work performed under the auspices of the U.S. Department of Energy by Lawrence Livermore National Laboratory under Contract DE-AC52-07NA27344. Abdul Awwal acknowledges the reviews performed by Steve Azevedo.

References

1. E. I. Moses, "Overview of the National Ignition Facility", *Fusion Science and Technology*, **54**, 361-366 (2008).
2. R. A. Zacharias, N. R. Beer, E. S. Bliss, et al., "Alignment and wavefront control systems of the National Ignition Facility," Opt. Eng. **43**, 2873-2884 (2004).
3. K. Wilhelmsen, A. Awwal, W. Ferguson, B Horowitz, V. Miller Kamm, C. Reynolds, "Automatic Alignment System For The National Ignition Facility", Proceedings of 2007 International Conference on Accelerator and Large Experimental Control Systems (ICALEPCS07), 486-490, Knoxville, Tennessee, (2007). http://accelconf.web.cern.ch/accelconf/ica07/PAPERS/ROAA02.PDF
4. C. A. Haynam, P. J. Wegner et al., "National Ignition Facility laser performance status," Appl. Opt. **46**, 3276-3303 (2007).
5. W. A. McClay III, A. A. S. Awwal, S. C. Burkhart, J. V. Candy, "Optimization and improvement of FOA corner cube algorithm," in *Photonic Devices and Algorithms for Computing VI*, edited by K. Iftekharuddin and A. A. S. Awwal,, Proc. of SPIE 5556 (SPIE Bellingham, WA, 2004), pp. 227-232.

6. A. A. S. Awwal, J. V. Candy, C. A. Haynam, C. C. Widmayer, E. S. Bliss, and S. C. Burkhart, "Accurate Position sensing of defocused beams using simulated beam templates," in *Photonic Devices and Algorithms for Computing VI*, edited by K. Iftekharuddin and A. A. S. Awwal, Proc. of SPIE 5556 (SPIE Bellingham, WA, 2004), pp. 233-242.
7. A. A. S. Awwal, "Automatic identification of templates in matched filtering," in *Photonic Devices and Algorithms for Computing VI*, edited by K. Iftekharuddin and A. A. S. Awwal,, Proc. of SPIE 5556 (SPIE Bellingham, WA, 2004), pp. 102-109.
8. A. A. S. Awwal, "Multi-object feature detection and error correction for NIF automatic optical alignment" in *Photonic Devices and Algorithms for Computing VIII*, edited by K. Iftekharuddin and A. A. S. Awwal,, Proc. of SPIE Vol. 6310 (SPIE Bellingham, WA, 2006), 63100Q.
9. A. A. S. Awwal Kenneth L. Rice, Tarek M. Taha, "Fast implementation of matched-filter-based automatic alignment image processing," Optics & Laser Technology, **41**, 193-197 (2009).
10. A. A. S. Awwal, Wilbert A. McClay, Walter S. Ferguson, James V. Candy, Thad Salmon, and Paul Wegner, "Detection and Tracking of the Back-Reflection of KDP Images in the presence or absence of a Phase mask," Appl. Opt. **45**, 3038-3048 (2006).
11. A. VanderLugt, "Signal Detection by Complex Spatial Filtering", IEEE Trans. Inf. Theory IT-10, 139-145 (1964).
12. J. L. Horner and J. Leger, "Pattern Recognition with Binary Phase-Only Filters", Appl. Opt. **24**, 609-611 (1985).
13. A. A. S. Awwal, M. A. Karim, and S. R. Jahan, "Improved Correlation Discrimination Using an Amplitude-Modulated Phase-Only Filter," Appl. Opt. **29**, 233-236 (1990).

14. M. A. Karim and A. A. S. Awwal, "Optical Computing: An Introduction", John Wiley, New York, NY, 1992.
15. K. M. Iftekharuddin, M. A. Karim, and A. A. S. Awwal, "Optimization of Amplitude Modulated Inverse Filter", *Mathematical and Computer Modeling*, Vol. 24, 103-112 (1996).
16. K. M. Iftekharuddin, M. A. Karim, P. W. Eloe, and A. A. S. Awwal, "Discretized Amplitude-Modulated Phase-Only filter", *Optics and Laser Technology*, **28**, 93-100 (1996).
17. Karl S. Gudmundsson, and A. A. S. Awwal, "Sub-Imaging Technique to Improve POF Search Capability", *Applied Optics*, **42**, 4709-4717 (2003).
18. B. V. K. Vijay Kumar and L. Hassebrook, "Performance measures for correlation filters," Appl. Opt. **29,** 2997-3006 (1990).
19. T. Wolf, B. Gutman, H. Weber, J. Ferre-Borrull, S. Bosch, and S. Vallmitjana, "Application of fuzzy-rule-based postprocessing to correlation methods in pattern recognition," Appl. Opt. **35**, 6955-6963 (1996).
20. R. S. Carpari, "Method of target detection in images by moment analysis of correlation peaks," Appl. Opt. **38**, 1317-1324 (1999).
21. P. C. Miller and R. S. Carpari, "Demonstration of improved automatic target-recognition performances by moment analysis of correlation peaks," Appl. Opt. **38**, 1325-1331 (1999).

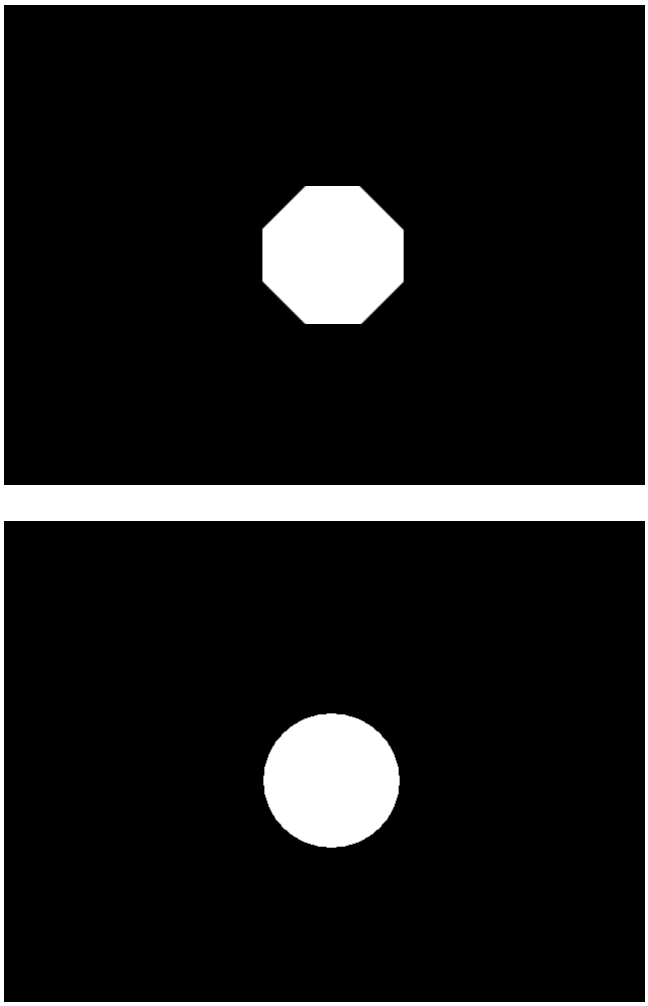

Fig. 1. Pedestal experiment performed by correlating the octagon and the circle shown above. The background is set at 0 and the white region set at 255.

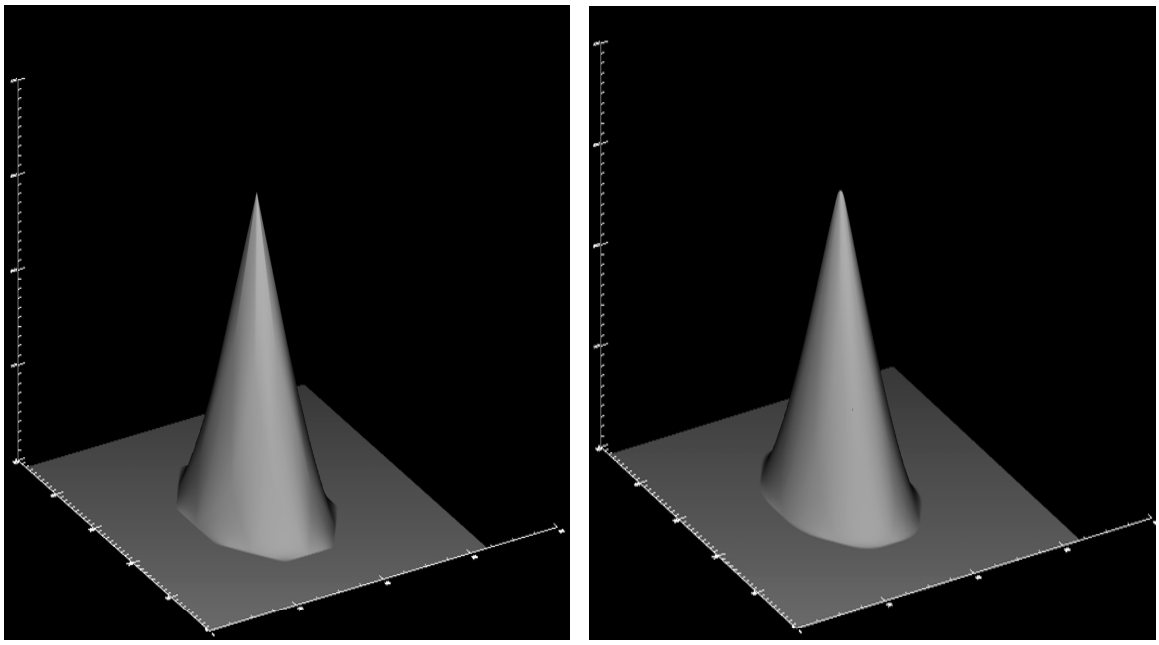

Fig. 2. Auto- and cross-correlation with CMF with the octagon as filter.

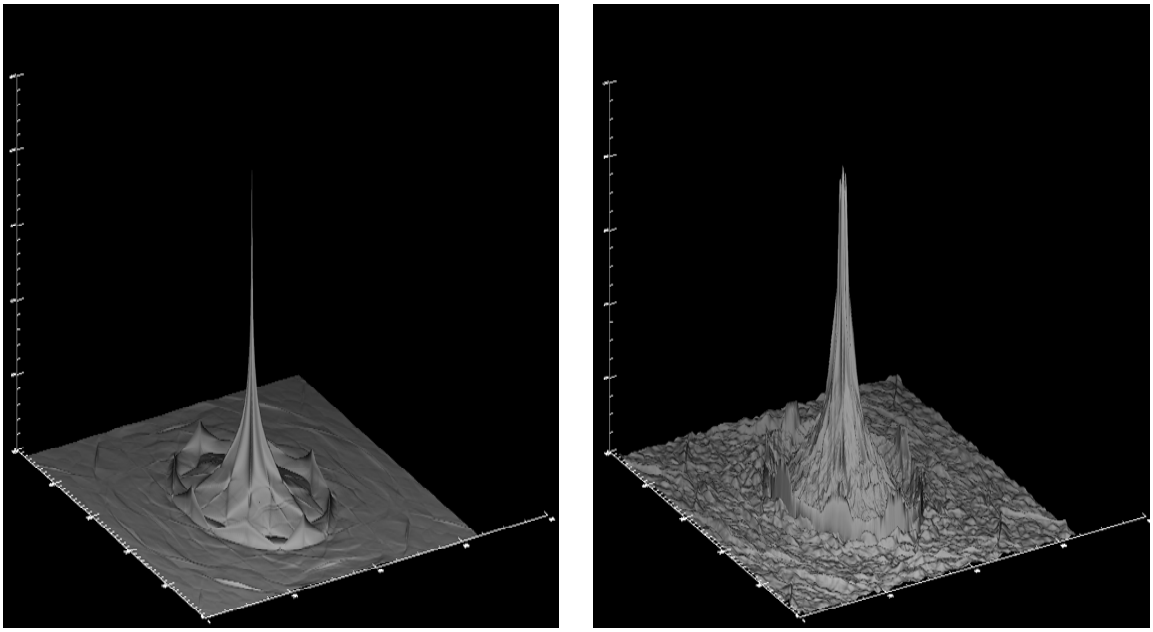

Fig. 3. Auto- and cross-correlation with AMPOF with the octagon as filter.

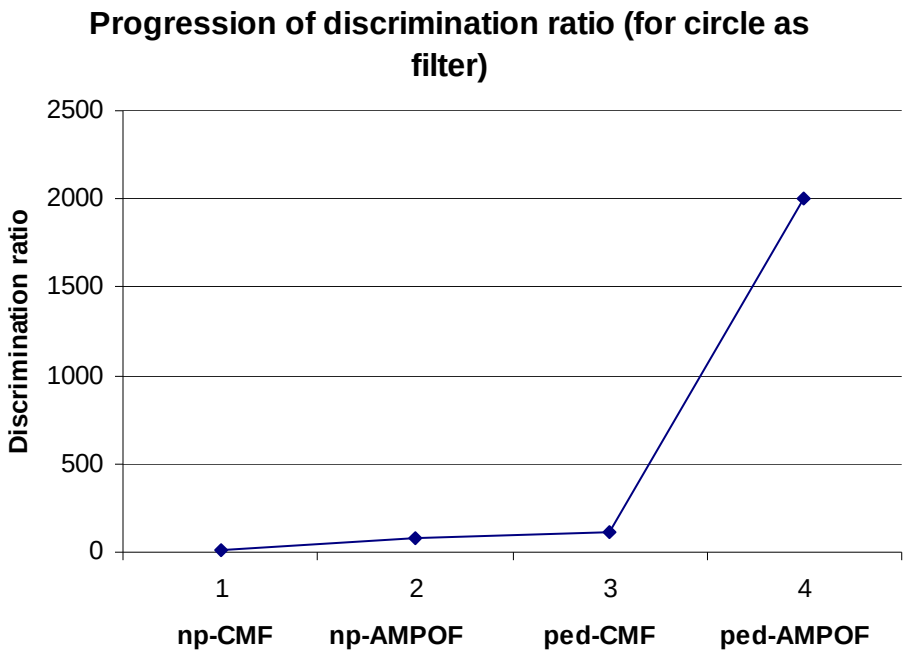

Fig. 4. Progression of discrimination showing 200 times improvement from normalized peak to pedestal of AMPOF.

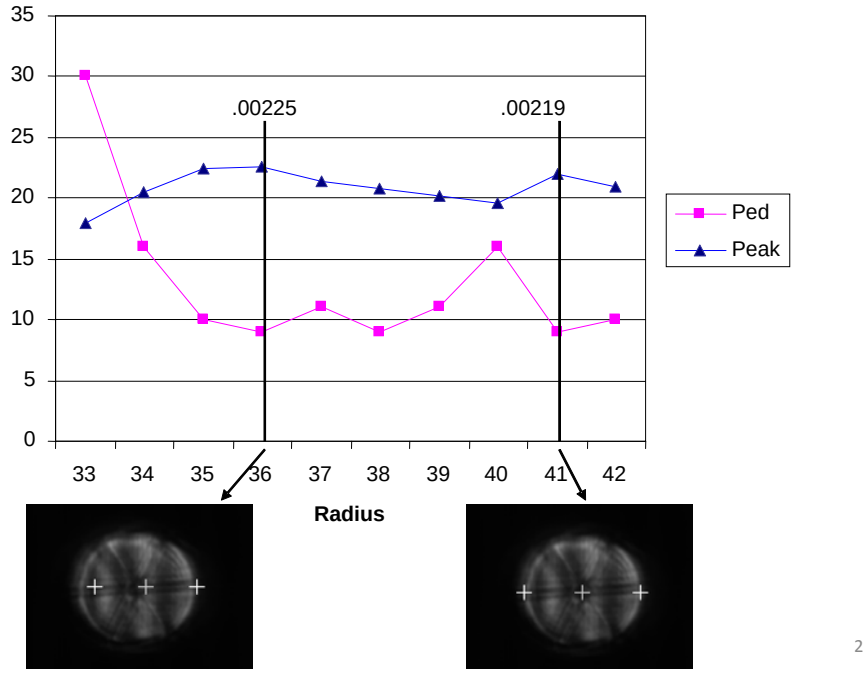

Fig. 5. The normalized peak and pedestal versus radius for corner cube pinhole image. When the maximum normalized peak at radius 36 is chosen the position estimation is biased towards the right, when a lower maxima at a minima pedestal at radius 41 is chosen the position is well centered.

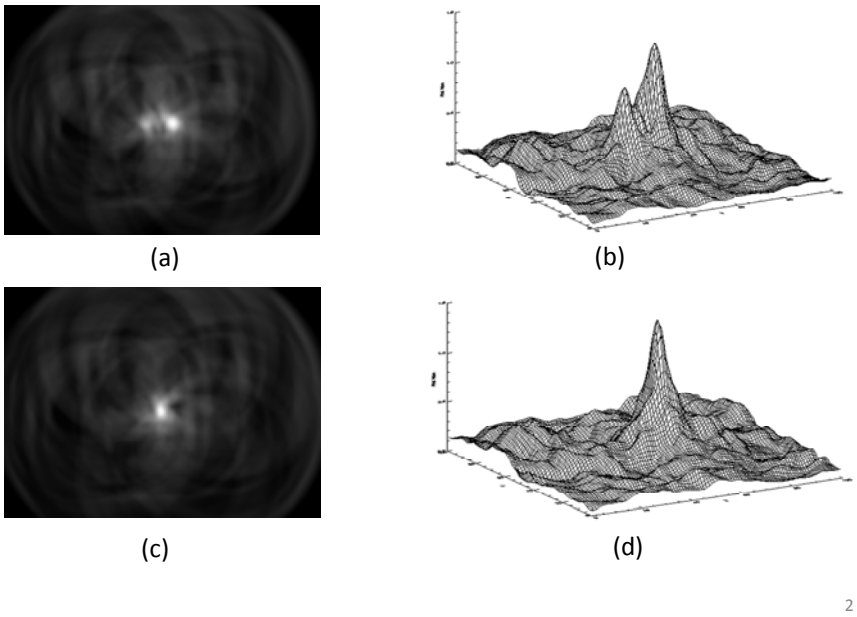

Fig. 6. (a) Correlation peak at radius 36 is maximum but with a double peak. (b) 3-d view of the correlation in a (c) correlation peak at radius 41. (d) 3-d view of (c) shows a single peak.

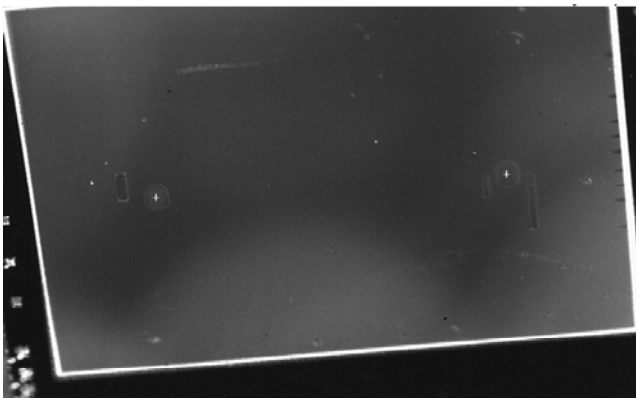

(a)

(b)

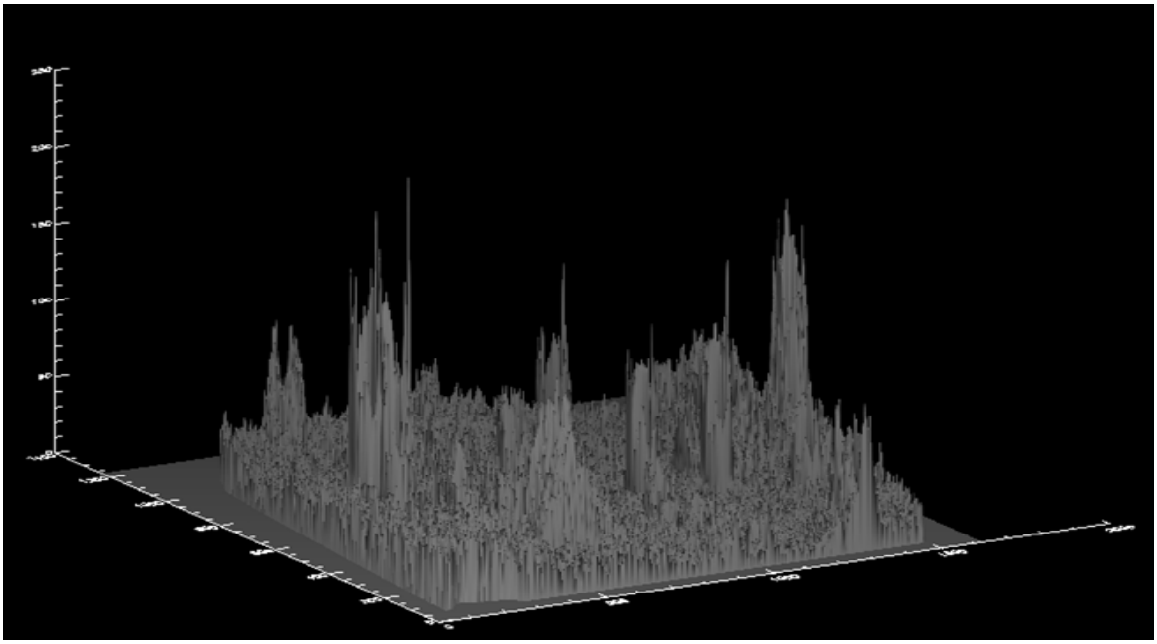

(c)

Fig. 7. (a) Active target images showing the fiducials to-be-detected, which are barely visible with extremely low contrast a side view of this image at an angle of nearly 15 degrees, is shown later in Fig. 10. (b) The template chosen from another real image. (c) Correlation plane output displaying a large number of peaks of which only two are valid.

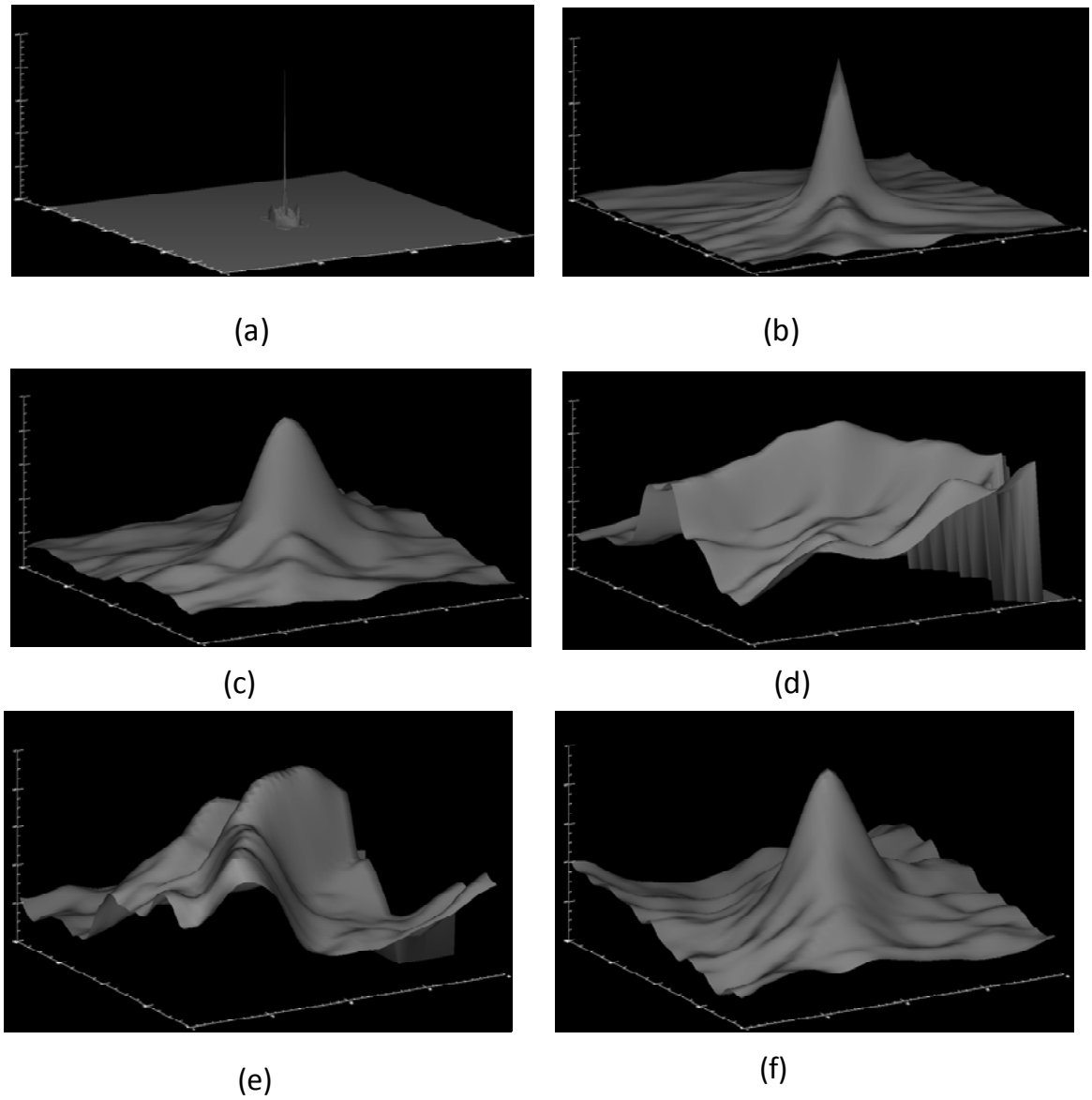

Fig. 8. (a) Total auto-correlation plane. (b) Segmented auto-correlation. (c) First detected maximum from the cross-correlation plane, matches with auto-correlation. (d) Second maximum does not match. (e) Third maximum does not match. (f) Fourth maximum matches with the self-correlation and is selected.

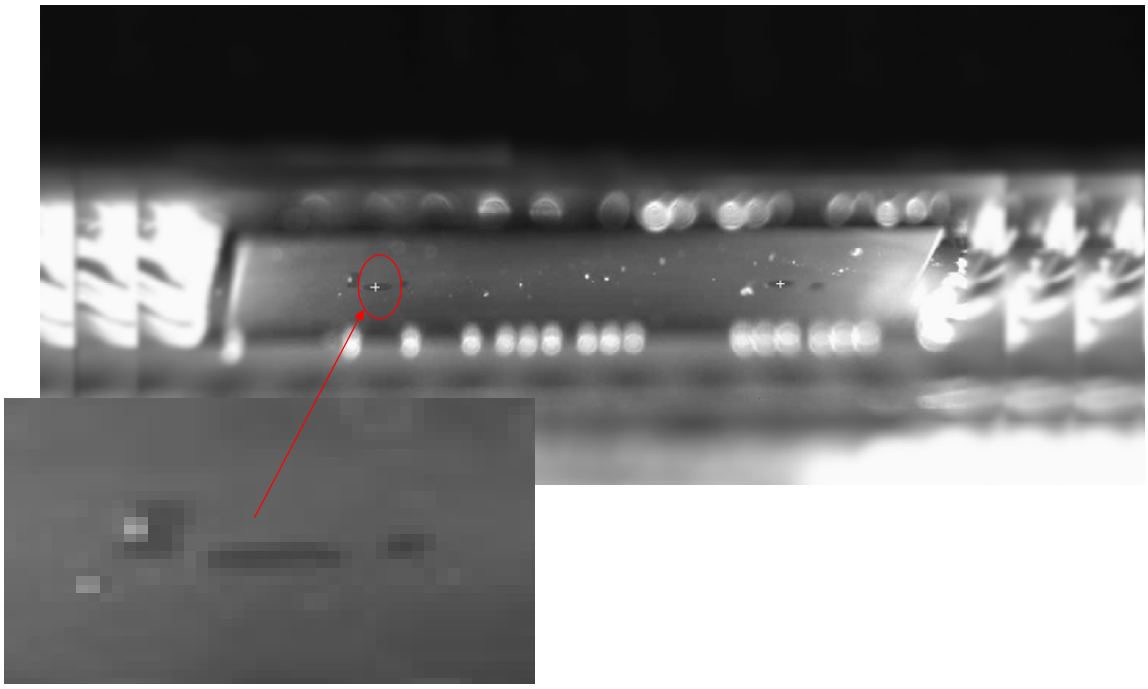

(a)

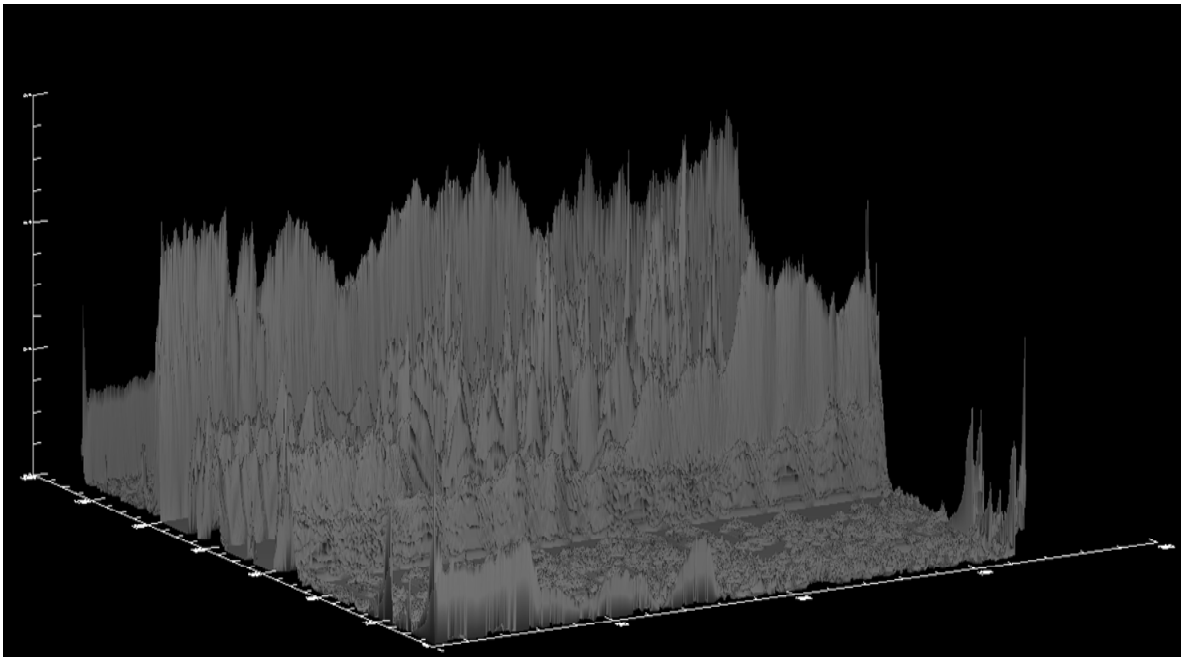

(b)

Fig. 9. (a) Active target side images showing extremely low contrast fiducials with very high-brightness noise. (b) The correlation plane output shows a large number of peaks due to high noise count.

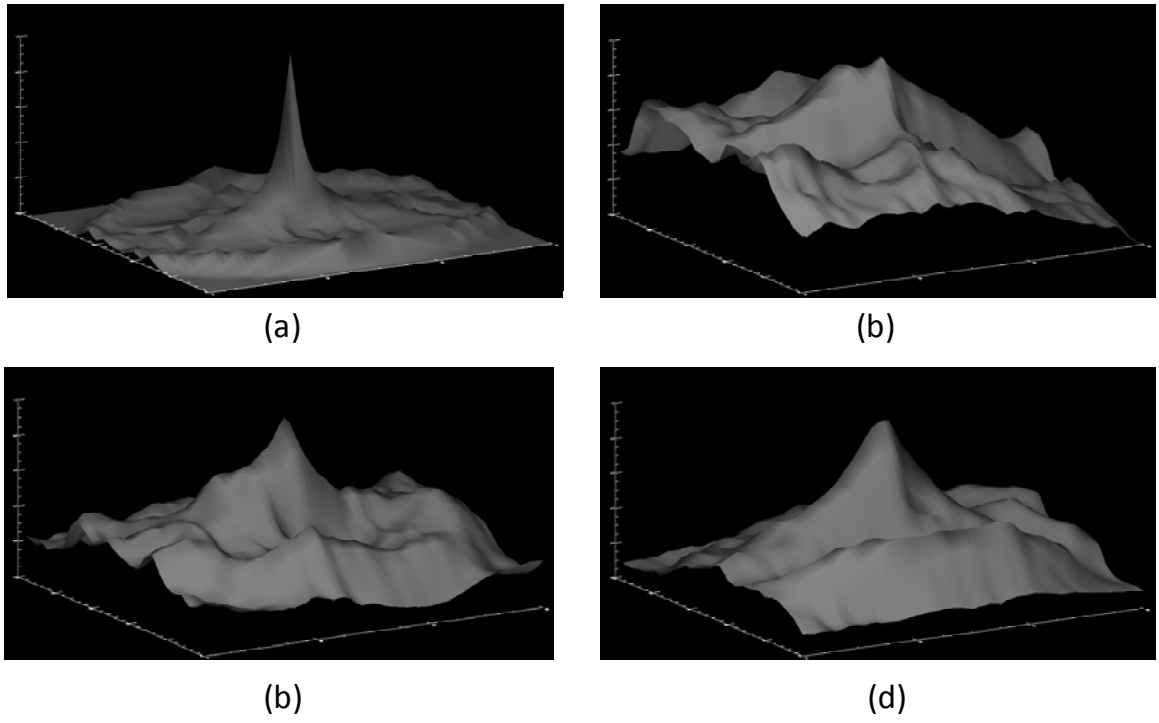

Fig. 10. (a) Segmented self-correlation. (b) First false peak. (c) Second peak a match, detected using the standard deviation of the product of inverse self-correlation. (d) Third peak, detected by the standard deviation of inverse method.

Table I. Comparison of pedestal versus normalized correlation peaks for AMPOF and CMF filters for the octagon and circle objects in terms discrimination ratio.

Exp. 1: CMF filter constructed from circle, the input objects are octagon and circle			
Features	Auto	Cross	Discrimination ratio
Pedestal at 0.5	9263	10844	17%
Pedestal at 0.9	349	741	112%
Normalized peak	7.03	6.34	9.8%
Absolute peak	3011	3011	0%

Exp. 2: CMF filter constructed from octagon, input objects are octagon and circle			
Features	Auto	Cross	Discrimination ratio
Pedestal at 0.5	10393	10844	4.3%
Pedestal at 0.9	407	741	82%
Normalized peak	6.32	6.34	0.31%
Absolute peak	3321	3011	9.3%

Exp. 3: AMPOF filter constructed from circle, input objects are octagon and circle			
Features	Auto	Cross	Discrimination ratio
Pedestal at 0.5	9	489	5300%
Pedestal at 0.9	1	21	2000%
Normalized peak	61.23	15.18	75%
Absolute peak	3335	1012	69%

Exp. 4: AMPOF filter constructed from octagon, input objects are octagon and circle			
Features	Auto	Cross	Discrimination ratio
Pedestal at 0.5	29	611	2006%
Pedestal at 0.9	1	97	9600%
Normalized peak	38.75	14.5	63%
Absolute peak	2309	905	69%

Exp. 5: CMF filter constructed from circle, input objects octagon and circle with noise 25			
Features	Auto	Cross	Discrimination ratio
Pedestal at 0.5	10150	11731	(17%) 15%
Pedestal at 0.9	379	783	(112%) 106%
Normalized peak	3.82	3.62	(9.8%) 5.2%
Absolute peak	2895	2988	(0%) -0.06% *

Exp. 6: CMF filter constructed from circle, input objects are octagon and circle with noise 100			
Features	Auto	Cross	Discrimination ratio
Pedestal at 0.5	(9263) 15741	(10844) 16329	(17%) 3.7%
Pedestal at 0.9	(349) 582	(741) 1005	(112%) 73%
Normalized peak	(7.03) 1.3	(6.34) 1.43	(9.8%) -10%*
Absolute peak	(3011) 2482	(3011) 2543	(0%) -2.5%*

Exp. 7: CMF filter constructed from circle, input objects octagon and circle with noise of amplitude 100			
Features	Auto	Cross	Discrimination ratio
Pedestal at 0.5	(9) 8	(489) 500	(5300%) 6150%
Pedestal at 0.9	(1) 1	(21) 8	(2000%) 700%
Normalized peak	(61) 12.56	(15) 4.8	(75%) 61.7%
Absolute peak	(3335) 2181	(1012) 784	(69%) 64%

Exp. 8: CMF filter constructed from octagon, input object octagon and circle with noise of amplitude 100			
Features	Auto	Cross	Discrimination ratio
Pedestal at 0.5	16160	18466	(4.3%) 14%
Pedestal at 0.9	613	1104	(80%) 82%
Normalized peak	1.43	1.19	(0.31%) 16%
Absolute peak	2808	2542	(9.3%) 9.4%

Exp. 9: AMPOF filter constructed from octagon, input object octagon and circle with noise of amplitude 100			
Features	Auto	Cross	Discrimination ratio
Pedestal at 0.5	31	704	(2006%) 2171%
Pedestal at 0.9	1	62	(9600%) 6100%
Normalized peak	10.5	3.9	(63%) 63%
Absolute peak	1616	652	(61%) 60%

Table II. Pedestal of Correlation Peak for detecting incorrect template

Beam number	Auto-correlation pedestal-in class (70.7% of maximum)	Cross-correlation Pedestal-out of class (70.7% of maximum)	Comments
Beam1	53		Noise free image beam1
Beam2		194	Different beam-line image
Beam3		524	Different beam-line image
Beam4		193	Different beam-line image
a100_i20_hw	115		Signal 100 interference noise 20
a100_n50	62		Signal 100 noise 50
a200_i10_hw	113		Signal 200 interference noise 10
a50_i10_hw	155		Signal 50 interference noise 10
a50_n50	143		Signal 50 and noise 50